Effect of Uncertain Hydraulic Conductivity on the Fate and Transport of BTEX Compounds at a Field Site

Guoping Lu

Earth Sciences Division
Lawrence Berkeley National Laboratory
MS 90-1116, 1 Cyclotron Road
Berkeley, CA 94720, USA.

Chunmiao Zheng

Department of Geological Sciences
University of Alabama
P.O. Box 870338
Tuscaloosa, AL 35487, USA.

Andrew Wolfsberg

Earth and Environmental Sciences Division
T003, EES-6
Los Alamos National Laboratory
Los Alamos, NM 87545, USA.

Submitted to *Journal of Hydrology*
January 18, 2002

Effect of Uncertain Hydraulic Conductivity on the Fate and Transport of BTEX Compounds at a Field Site

Guoping Lu, *Chunmiao Zheng*, and *Andrew Wolfsberg*

Abstract

A Monte Carlo analysis was conducted to investigate the effect of uncertain hydraulic conductivity on the fate and transport of BTEX compounds (benzene, toluene, ethyl benzene, and xylene) at a field site on Hill Air Force Base, Utah. Microbially mediated BTEX degradation has occurred at the site through multiple terminal electron-accepting processes, including aerobic respiration, denitrification, Fe(III) reduction, sulfate reduction, and methanogenesis degradation. Multiple realizations of the hydraulic conductivity field were generated and substituted into a multispecies reactive transport model developed and calibrated for the Hill AFB site in a previous study. Simulation results show that the calculated total BTEX masses (released from a constant-concentration source) that remain in the aquifer at the end of the simulation period statistically follow a lognormal distribution. In the first analysis (base case), the calculated total BTEX mass varies from a minimum of 12% less and a maximum of 60% more than that of the previously calibrated model. This suggests that the uncertainty in hydraulic conductivity can lead to significant uncertainties in modeling the fate and transport of BTEX. Geometric analyses of calculated plume configurations show that a higher BTEX mass is associated with wider lateral spreading, while a lower mass is associated with longer longitudinal extension. More BTEX mass in the aquifer causes either a large depletion of dissolved oxygen (DO)

and NO_3^-, or a large depletion of DO and a large production of Fe^{2+}, with moderately depleted NO_3^-. In an additional analysis, the effect of varying degrees of aquifer heterogeneity and associated uncertainty is examined by considering hydraulic conductivity with different variances and correlation lengths. An increase in variance leads to a higher average BTEX mass in the aquifer, while an increase in correlation length results in a lower average. This observation is explained by relevant partitioning of BTEX into the aquifer from the LNAPL source. Although these findings may only be applicable to the field conditions considered in this study, the methodology used and insights gained are of general interest and relevance to other fuel-hydrocarbon natural-attenuation sites.

Key words: uncertainty, hydraulic conductivity, transport, BTEX, attenuation.

1. Introduction

In recent years, natural attenuation has emerged as a low-cost option for remediation of hydrocarbon contaminants (USEPA, 1997; NRC, 2000; Bekins et al., 2001). To apply natural attenuation as a remediation strategy successfully under field conditions, we need to understand how the inherent uncertainty in hydraulic conductivity affects the natural attenuation process.

Several investigations have revealed the importance of aquifer heterogeneity to biodegradation of hydrocarbons. Patrick (1986) conducted a natural gradient tracer experiment in the Borden aquifer in Canada, using a pulse tracer solution containing dissolved benzene, toluene, and xylenes. Both aerobic biodegradation and retardation were shown to result in mass loss for all organic solutes. The availability of dissolved oxygen was determined to be a primary factor controlling the mass loss rates. Oxygen was inferred to be transported to the organic solutes by advection and dispersion from high hydraulic conductivity layers, indicating the importance of aquifer heterogeneity. Widdowson et al. (1987) also suggested that aquifer structure may play a role in biodegradation, based on the results of a two-dimensional numerical model.

MacQuarrie and Sudicky (1990) examined the migration of a biodegradable organic toluene plume emanating from a pulse source in a shallow aquifer, where natural dissolved oxygen was the only electron acceptor. The dissolved organic and oxygen distributions were demonstrated to be highly irregular in heterogeneous aquifers because of small-scale groundwater velocity variations. They studied the rate of mass

loss, and position and spreading rate of the organic plume. James and Oldenburg (1997) investigated the uncertainty of simulated trichloroethylene (TCE) plumes resulting from parameter uncertainty and variation in the conceptual model by both a linear and Monte Carlo analyses. Literature related to modeling the fate and transport of benzene, toluene, ethyl benzene, and xylene at field sites can be found in several recent studies, including Essaid et al. (1995), Borden et al. (1997), and Brauner and Widdowson (2001).

To quantify the uncertainty about aquifer heterogeneity, there are two approaches that can be taken with the simulated hydraulic conductivity realizations. One would be to check each one and accept it only if the RMS error for simulated heads and observed heads were within some specified threshold. Such a threshold, however may be poorly defined or arbitrary. The other approach is to utilize all realizations of hydraulic conductivity assuming that the variability in the transport results from the Monte Carlo simulations falls within the uncertainty associated with the calibrated flow and transport model. Such an approach is only concerned with the ensemble statistics rather than any particular realization. In this study, the latter approach is used.

This study addresses the influence of uncertain hydraulic conductivity (K) on the fate and transport of BTEX at a field site on the Hill Air Force Base (AFB), Utah. We will use the multispecies reactive transport model developed and calibrated in a previous study (Lu et al., 1999) as the basis for comparison. We will also examine the impact of uncertainty in the K field on the results of multispecies reactive transport modeling by considering multiple realizations of the K field under different variances and correlation lengths. The variation in simulation results provides an effective

measure of how aquifer heterogeneity and associated uncertainties affect the fate and transport of BTEX compounds.

2. Study Site

The Hill AFB is located on a bench formed by fluvial-deltaic basin fill deposits of the ancient Weber River, on the southeast edge of the Great Salt Lake Basin. The study site is a petroleum, oil, and lubricant (POL) facility in the southwestern corner of the base (Figure 1). The unconfined aquifer beneath this site consists of poorly to moderately sorted, silty fine-grained sands that coarsen downward into moderately sorted medium-to-coarse-grained sands. These sands range in thickness from approximately 3 to 22 feet (0.9 to 6.7 m) with the shallow saturated zone occurring within these sands. The shallow saturated zone is typically less than 3 feet (0.9 m) thick. Abruptly overlying the sands is a clayey silt to silty clay interval, ranging in thickness from approximately 4 to 15 feet (1.2 to 4.6 m). Underlying the sandy layer is a sequence of thinly interbedded clay to silty-clay and fine-grained sand and silt, which appears to act as a barrier to the vertical migration of flow and contaminants (Figure 2). The measured hydraulic conductivity of the medium-to-coarse-grained sands in the shallow saturated zones ranges from 0.43 to 53 ft/day (0.13 to 16.15 m/day) with an average value of 19 ft/day (5.79 m/day), based on 11 measurements from 5 boreholes (Wiedemeier et al., 1995).

At the POL facility, a 1,000 gallon (3.8 m^3) underground storage tank (UST 870) was used to store condensed and off-specification jet fuel JP-4. The tank was excavated and removed in May 1991, and upgraded with a new double-walled steel UST serving

the same purpose. Soil and groundwater at the site were found to be contaminated during removal of UST 870. Some mobile, light nonaqueous phase liquid (LNAPL) was present in several monitoring wells and piezometers at the site. The areal extent of the mobile LNAPL contamination was approximately 225,000 square feet (20,903.2 m^2).

A review by Lu et al. (1999) of available data for 20 field monitoring campaigns between August 1992 and April 1994 (Wiedemeier et al., 1995) revealed that LNAPL at this site seems to follow a distinct cyclic pattern; its areal extent is smaller from May to December than from January to April. This changing pattern may be the result of the interaction between clayey silt and silty clay lenses at the site, and of seasonal recharge events. In the flow field, a lower hydraulic gradient occurred in the lower (northwestern) side around borehole CPT 33 (Figure 1), which is resulted from a generally higher elevation in that local area of the aquifer (Lu et al., 1999). This causes lateral spreading of the plumes to the upper side of the flow field, as described later in the Section 6 base case.

3. Reactive Transport Model

Lu et al. (1999) developed a reactive transport model to simulate natural attenuation of BTEX compounds at the POL site on the Hill AFB based on the following set of governing transport equations:

$$R_{HC}\frac{\partial[\mathrm{BTEX}]}{\partial t}=\frac{\partial}{\partial x_i}\left(D_{ij}\frac{\partial[\mathrm{BTEX}]}{\partial x_j}\right)-\frac{\partial\left(v_i[\mathrm{BTEX}]\right)}{\partial x_i}+\frac{q_s}{\varphi}[\mathrm{BTEX}]_s+r_{HC} \qquad (1)$$

$$R_{EA}\frac{\partial[EA]}{\partial t}=\frac{\partial}{\partial x_i}\left(D_{ij}\frac{\partial[EA]}{\partial x_j}\right)-\frac{\partial(v_i[EA])}{\partial x_i}+\frac{q_s}{\varphi}[EA]_s+r_{EA} \quad (2)$$

where R is the retardation factor for various species, r is the biodegradation rate term, D_{ij} is the dispersion coefficient tensor, v_i is the groundwater seepage velocity, q_s is the fluid sink/source term, and φ is the porosity. The concentrations of various species are represented by a square bracket around an appropriate notation for the respective species.

A kinetic model was used by Lu et al. (1999) to describe hydrocarbon biodegradation as an oxidation-reduction process in which the hydrocarbon (BTEX) is oxidized and electron acceptors (e.g., O_2, NO_3^-, Fe^{3+}, SO_4^{-2}, or CO_2) are reduced sequentially. In the sequential degradation of fuel hydrocarbon under aerobic, denitrifying, iron-reducing, sulfate-reducing, and methanogenic conditions, the kinetics of hydrocarbon decay were assumed to be first order with respect to the hydrocarbon concentration. This can be expressed as

$$r_{BTEX,O_2}=-k_{O_2}[BTEX]\frac{[O_2]}{K_{O_2}+[O_2]} \quad (3)$$

$$r_{BTEX,NO_3^-}=-k_{NO_3^-}[BTEX]\frac{[NO_3^-]}{K_{NO_3^-}+[NO_3^-]}\frac{K_{i,O_2}}{K_{i,O_2}+[O_2]} \quad (4)$$

$$r_{BTEX,Fe^{2+}}=-k_{Fe^{3+}}[BTEX]\frac{[Fe^{3+}]}{K_{Fe^{3+}}+[Fe^{3+}]}\frac{K_{i,O_2}}{K_{i,O_2}+[O_2]}\frac{K_{i,NO_3^-}}{K_{i,NO_3^-}+[NO_3^-]} \quad (5)$$

$$r_{BTEX,SO_4^{-2}} = -k_{SO_4^{-2}}[BTEX]\frac{[SO_4^{-2}]}{K_{SO_4^{-2}}+[SO_4^{-2}]}\frac{K_{i,O_2}}{K_{i,O_2}+[O_2]}\frac{K_{i,NO_4^-}}{K_{i,NO_4^-}+[NO_4^-]}\frac{K_{i,Fe^{3+}}}{K_{i,Fe^{3+}}+[Fe^{3+}]} \quad (6)$$

$$r_{BTEX,CH_4} = -k_{CH_4}[BTEX]\frac{[CO_2]}{K_{CH_4}+[CO_2]}\frac{K_{i,O_2}}{K_{i,O_2}+[O_2]}\frac{K_{i,NO_3^-}}{K_{i,NO_3^-}+[NO_3^-]}\frac{K_{i,Fe^{3+}}}{K_{i,Fe^{3+}}+[Fe^{3+}]}\frac{K_{i,SO_4^{-2}}}{K_{i,SO_4^{-2}}+[SO_4^{-2}]} \quad (7)$$

where r_{BTEX,O_2} is the hydrocarbon destruction rate [$ML^{-3}\,T^{-1}$] utilizing oxygen, r_{BTEX,NO_3^-} is the destruction rate utilizing nitrate, $r_{BTEX,Fe^{2+}}$ is the destruction rate utilizing Fe^{3+} (or producing Fe^{2+}), $r_{BTEX,SO_4^{-2}}$ is the destruction rate utilizing sulfate, r_{BTEX,CH_4} is the destruction rate via methanogenesis, $[O_2]$ is the oxygen concentration [ML^{-3}], k_{O_2} is the first-order degradation rate constant for hydrocarbon utilizing oxygen as the electron acceptor [T^{-1}], K_{O_2} is the Monod half saturation constant [ML^{-3}], K_{i,O_2} is the oxygen inhibition constant [ML^{-3}]; similar nomenclature is used for other species.

In equation (1), the total rate of hydrocarbon transformation via destruction processes, r_{HC}, can be represented as

$$r_{HC} = r_{HC,O_2} + r_{HC,NO_3^-} + r_{HC,Fe^{2+}} + r_{HC,SO_4^{-2}} + r_{HC,CH_4} \quad (8)$$

In equation (2), rates of electron acceptor utilization or product formation, r_{EA}, for O_2, NO_3^-, Fe^{2+}, SO_4^{2-}, and CH_4 are given by the corresponding rates of hydrocarbon

destruction, multiplied by the appropriate yield coefficients. More detailed discussions on the formulation and limitation of the model can be found in Lu et al. (1999).

The reactive transport model described above was solved using the RT3D code (Clement, 1998), which is a generalized multispecies reactive package coupled with the modular transport code MT3D (Zheng, 1990). The flow solution required by the transport model was solved by the MODFLOW code (McDonald and Harbaugh, 1988). Basic setup of this model is summarized as bellow. (Interested readers can find more details from the calibrated model by Lu et al. [1999]). The model domain is 3,300 ft (1,006 m) along the flow direction, 1,700 ft (518 m) transverse to the flow direction, and discretized as 30 columns and 20 rows with a grid spacing of 110 by 85 ft (34 by 26 m). In the vertical dimension, the model consists of a single, unconfined layer.

Initial and boundary conditions for the model were defined by field data of LNAPL, BTEX, electron acceptors, or reduced products. In according with data collected in July–August 1993 and July 1994 (Wiedemeier et al., 1995), the natural attenuation simulations were conducted for a period of 365 days, from August 1993 to July 1994. To represent the seasonal variation of the LNAPL source, the total simulation time of 365 days was divided into three stress periods of 162, 106, and 97 days, respectively. The LNAPL source was modeled by assigning field-measured concentration for each stress period. This constant-concentration approach to modeling the LNAPL source is expected to more realistically reflect the partitioning of BTEX mass from the source. BTEX mass dissolved into the aquifer is thus related with concentration gradient, which is affected by hydraulic conductivity field. The first-order biodegradation rate constants, estimated from model calibration, are 0.051, 0.031, 0.005, 0.004, and 0.002

day^{-1}, respectively, for BTEX reactions with dissolved oxygen (DO), nitrate, ferric iron (III), sulfate, and carbon dioxide. The sensitivity analysis shows that the hydraulic conductivity is the most sensitive input parameter of the model (Lu et al., 1999).

No sorption was included in the model owing to very low measured total organic carbon contents for the shallow saturated zone (Wiedemeier et al., 1995). Because the saturated thickness of the unconfined aquifer is very small, flow simulation is vulnerable to a numerical problem that causes many model cells to go "dry" and to be prematurely removed from calculation as the head iterates toward a converged solution. To circumvent this problem, we the saturated thickness of the calibrated model (Lu et al., 1999) in all the new simulations conducted for the Monte Carlo analysis by treating the aquifer as a confined model layer. The specification of the water-table aquifer as a confined aquifer is presumed to approximate field conditions. Thus, the conclusions from this study should be considered applicable only to confined aquifer conditions.

4. Generation of Hydraulic Conductivity Distributions

Measured K values around the plume area range from 0.31 to 16.01 m/day ($\ln K = -1.16$ to 2.77, with a mean of 0.96 and a variance of 2.73) (Tables 1, 2). The mean and variance of the measured values were used to generate multiple realizations of the K field to represent the uncertainty there. The turning bands method (TUBA) code (Zimmerman and Wilson, 1990) was used as the random field generator. A total of 200 realizations were generated for each case study. (This number is arbitrary and is meant to keep within a practically operational quantity; the actual number of realizations used in the analysis was statistically determined.) Total mass of BTEX at

the end of each simulation was summed and averaged, and the total required realizations were obtained when the average mass yielded very small fluctuations. In our base case runs, 120 realizations were considered to have met the above statistical requirement.

Two cases were considered in this study. In the first case (base case), 120 realizations were used for simulation. These realizations use the same mean and variance as those of measured K values (Table 2). The K field was assumed to follow a Gaussian semi-variogram model, with a correlation length equal to four times the grid spacing along both column and row directions. The above total number of realizations is the number of simulations required for a stable mean value of calculated BTEX masses remaining in the aquifer at the end of simulations. In the second case (extended case), several groups, each of which contains all 200 realizations, have the same mean as that of measured K values, but with different variances and correlation lengths. The base case investigates how the estimated uncertainty in the K field affects the results of the reactive transport model for the study site, in comparison with those of the calibrated model (Lu et al., 1999). The extended case attempts to quantify the relationship between the model results and varying degrees of uncertainty in the K field.

5. Quantification of Plume Characteristics

Flow simulation using MODFLOW and reactive transport simulation using RT3D were conducted for each K realization. At the end of the 1-year simulation period from August 1993 to July 1994, the resulting concentrations of BTEX, DO, nitrate, ferrous

iron, sulfate, and methane were combined with porosity and saturated aquifer thickness to obtain the mass of each species in the aquifer. The configuration of each plume was delineated using the concentration contour line of 0.05 mg/L as the outer boundary.

The shape of the plume is described using the elongation ratio (R_e), introduced by Schumm (1956) for stream shapes:

$$R_e = \frac{D_c}{L} \tag{9}$$

where D_c is the diameter of a circle with the same area as that of the plume, and L is the maximum length of the plume along a line approximately parallel or transverse to the regional flow direction. The more elongated the plume, the smaller the R_e value.

Another factor used in the analysis is the shape ratio (R_s):

$$R_s = \frac{\pi D_c}{c_p} \tag{10}$$

where c_p is the perimeter of the plume. An ideal shape (such as a circle) has a value of $R_s = 1$. The more irregular the plume shape is, the smaller the R_s value becomes.

The last factor is the coefficient of skewness:

$$S_k = \frac{\sum_{i=1}^{N} (\mathrm{y_i} - \bar{y})^3}{\mathrm{N} \quad s^3} \tag{11}$$

where y_i is the location of a cell on the plume perimeter, $\bar{y}$ the centroid location of a plume area used as the reference (with the central line along the BTEX plume in the calibrated model used as the reference axis), N is the number of model cells making up the plume perimeter, and s is the standard deviation of the location values for these model cells.

To establish the relationship between the BTEX mass and those of DO, nitrate, ferrous iron, sulfate, and methane, we applied the concept of fuzzy entropy (Zadeh, 1968) to measure the associated uncertainty of the system. Entropy is defined as follows. Let x be a random variable that takes values $x_{i1}, \cdots, x_{in}$ with their respective probabilities $P(i1), \cdots, P(in)$, where $x = \{$[BTEX], [DO], [nitrate], [ferrous iron], [sulfate], [methane]$\}$ in this case. (A specific value for x_i could be a descriptor such as high, medium, or low.) Then the entropy of x—or, more properly, the entropy of the distribution $P = \{P(1), \cdots, P(n)\}$— is given by

$$Entropy(x) = -\sum_{k=1}^{n} P(k) \log_2 P(k) \tag{12}$$

where k is the number of class categories (k is 6 for this study). If the values of a random variable fall within a single category, the entropy is zero, and no further information is required for grouping (i.e., all the data values can be classified into one group). Membership of individuals (random variables) is described in terms of either mass or mass differences with respect to the calibrated model. Values for BTEX mass can be classified as {high, medium, low}, and mass difference for DO, nitrate, ferrous iron, sulfate, and methane can be {large, medium, small}, or {large, small}.

6. Base Case

The BTEX mass remaining in the aquifer at the end of the simulation period was used to quantify the behavior of the reactive transport model in response to natural attenuation. The distribution of the BTEX mass for all 120 hydraulic conductivity realizations with the same mean, variance, and correlation length was assembled as a

measure of the uncertainty in model results caused by the uncertainty in hydraulic conductivity. The distributions of other plume characteristics, including elongation and shape ratios, were also evaluated to examine how they are affected by the uncertainty in hydraulic conductivity. Finally, the BTEX mass was statistically related to the consumption of electron acceptors to illustrate the influence of hydraulic conductivity on the multispecies dynamics of the natural attenuation process.

The histogram of the calculated total BTEX mass in the aquifer from all 120 runs at the end of the 1-year simulation period is shown in Figure 3. The plot is characteristic of a lognormal distribution. Calculated mass ranges from a minimum of 12% less than and a maximum of 60% more than that of the previously calibrated model (Lu et al., 1999). The histogram skews to the left, with a skewness coefficient of 1.34. Average mass is 36.57 kg, or 9.8% larger than the 33.30 kg from the calibrated model. This difference suggests that the BTEX mass was underestimated in the calibrated model because the uncertainty in the K field was not considered. The difference between the maximum and minimum of the calculated total BTEX masses is 24.11 kg, which is 72.4% of the mass in the calibrated model. Standard deviation for the calculated BTEX masses is 13.9 kg. Overall, the uncertainty in the K field results in significant uncertainty in modeling natural attenuation of BTEX.

In Table 3, the range, mean and standard deviation of calculated masses for BTEX and other species are compared with those of the calibrated model. The values in Table 3 are expressed in terms of the percentage of difference from the corresponding values in the calibrated model. Calculated average masses of electron acceptors DO, nitrate, and sulfate are less than that of the calibrated model, indicating more consumption (i.e.,

they are more depleted, on average, than in the calibrated model). Calculated average masses of end products, ferrous iron and methane, on the other hand, are larger than that of the calibrated model, suggesting that more of them are produced from biodegradation.

The BTEX masses are found to correlate well with plume areas delineated using the 0.05 mg/L contour line. The larger the plume area, the higher the BTEX mass. The histogram of calculated BTEX plume areas for 120 simulations, shown in Figure 4, follows a lognormal pattern. The average plume area is 8,500 m^2, 12% larger than that of the calibrated model.

The geometric configuration of the BTEX plume is the combined effect of advection, dispersion, and degradation. A closer examination of the plume configuration could reveal useful information on the role of aquifer heterogeneity in affecting the fate and transport of BTEX compounds. For this purpose, shape descriptors including longitudinal and transverse elongation and roundness, are examined. In the longitudinal direction along the flow direction, the average elongation ratio has a higher value than that of the calibrated model, indicating that the plumes tend to be shorter than those determined for the calibrated model (Figure 5). However, a more elongated plume (indicated by a smaller value of longitudinal elongation ratio) generally leads to less BTEX mass in the aquifer. This may be because the less elongated the plume, the less likely channelization will occur, and thus BTEX mass will be more effectively dissolved into the groundwater and spread to a wider area. In the transverse direction, the elongation ratio has a lower value than that of the

calibrated model (Figure 6), suggesting that calculated plumes for the Monte Carlo analysis are generally wider than that of the calibrated model.

The shape ratio measures the irregularity of a plume's boundary; a plume of a circular shape has a shape ratio close to 1. The BTEX plumes resulting from the Monte Carlo simulations have a higher average shape ratio than that of the calibrated model (Figure 7), implying that the plumes are overall more circular than that of the calibrated model. This is consistent with the observation (based on an analysis of elongation ratios) that the calculated plumes for the Monte Carlo analysis are shorter longitudinally but wider transversely than those of the calibrated model.

Larger lateral spreading for the plumes calculated in the Monte Carlo analysis result from a lower hydraulic gradient, caused by higher elevation in a local area of the aquifer (lower flow field around borehole CPT 33 (Figure 1)) (Lu et al., 1999). The concept of skewness can be used to quantify the variations in lateral plume displacement caused by variations in the K field. Plume displacement relative to the calibrated model was characterized by the skewness coefficient. The central line along the calibrated BTEX plume (parallel to the x-axis in the general flow direction) was used as reference. Plumes that skewed to the lower side of the flow field have negative skewness coefficients, corresponding to smaller plume areas; plumes that skewed to the upper side of the flow field have positive skewness coefficients and larger plume areas. A negatively skewed plume tends to have less spreading, while a positively skewed plume tends to be more widely spread (Figure 8). The plumes show an asymmetric distribution and are more frequently skewed to the upper half of the flow domain.

The relationship between the BTEX mass and masses of DO, nitrate, sulfate, Fe(III), and methane was characterized using fuzzy entropy (Figure 9). The BTEX mass was grouped into three categories: high (total BTEX mass ≥37 kg), low(<34 kg), and medium (≥ 34 and <37 kg). The mass of DO, nitrate, ferrous iron, sulfate and methane was expressed in terms of mass differences relative to the calibrated model. The first feature used for relationship testing is "DO difference" with respect to the calibrated model, which was divided into three categories: large (difference ≥100 kg), medium (≥ 30 and <100 kg), and small (<30 kg). "NO_3^- difference" was also divided into three categories: large (difference ≥ 90 kg), small (<30 kg), and medium (≥ 30 and < 90 kg). "Fe^{2+} difference" was separated into two categories: large (difference ≥ 100 kg) and small (<100 kg). The entropy of the system before testing is 1.524. The information gain by testing DO difference is 1.003, indicating that BTEX can be classified by DO difference.

Further testing of NO_3^- and/or Fe^{2+} also yields other significant information. Sulfate and methane were not substantial features for relationship testing, because of their low reaction rates and sulfate's high background concentration. This is consistent with the finding from a sensitivity analysis that sulfate and methane have the lowest sensitivity (Lu et al., 1999). Several generalized rules were constructed from Figure 9 for the relationship between BTEX mass and DO, NO_3^-, and Fe^{2+}. A combination of large DO and NO_3^- mass difference results from a high BTEX mass in the aquifer. A high BTEX mass could also lead to a large DO and Fe^{2+} mass difference with a moderate NO_3^- mass difference. A low BTEX mass in the aquifer could end up with small difference of both DO and Fe^{2+}.

7. Extended Case

For the base case, the variance of the random lnK fields was set to 2.73 (Tables 1, 2) based on measured K values, and the correlation length was assumed to be four times the grid spacing. To quantify how the natural attenuation model responds to varying degrees of uncertainty in the K field, we generated seven K groups, each of which contains 200 realizations, for the extended case, with variances of 1, 2, 2.73, and 4 and correlation lengths of 1.0, 1.5, and 2 times that of the base case. Figure 10 shows the mean and variance of the calculated BTEX mass for each simulation group with respect to the variance and correlation length of the random K realizations generated for each group. The vertical axis represents the mean BTEX mass, and the three-dimensional contour surface represents the variance of BTEX masses.

The mean BTEX mass in the aquifer increases as the K variance increases for any given correlation length, but decreases as the correlation length increases for any given K variance. A higher K variance indicates a higher degree of heterogeneity and greater uncertainty. This appears to result in a higher average BTEX mass released from the LNAPL source and remaining in the aquifer. On the other hand, a larger correlation length for the K field resulted in a lower average BTEX mass released from the LNAPL source and remaining in the aquifer. This observation is resulted from the partitioning of BTEX mass from DNAPL sources. Note that these findings concerning the relationship between the BTEX mass and the variance and correlation length of the K field are obtained for this study under the constant-concentration boundary conditions, which are more appropriate for field characterization, and thus may not be applicable to other types of flow and transport conditions.

8. Summary and Conclusions

A multispecies reactive transport model was developed and calibrated in a previous study (Lu et al., 1999) to describe the sequential degradation of BTEX utilizing multiple electron acceptors, including oxygen, nitrate, iron and sulfate, and via methanogenesis, at the Hill AFB site. The model was used in this study to investigate the fate and transport of BTEX compounds under uncertain hydraulic conductivity.

The uncertainty associated with hydraulic conductivity was represented by multiple equally likely realizations of a random field. The mean and variance of the logarithmic hydraulic conductivity values (lnK) for the Hill AFB site were estimated to be 0.96 m/day and 2.73, respectively. The correlation length was assumed to be four times the grid spacing. Each hydraulic conductivity realization was used to replace the hydraulic conductivity distribution used in the previously calibrated model. The model simulates multispecies transport for one year, from August 1993 to July 1994, based on the initial conditions estimated from the August 1993 data.

The calculated total mass of dissolved BTEX in the aquifer approximates lognormal distribution. The mean value from 120 realizations used in the base case is 36.57 kg, or 9.8% larger than 33.30 kg for the calibrated model. The standard deviation is 4.60 kg with a minimum of 29.32 kg and a maximum of 53.43 kg, yielding a range of 24.11 kg, or 72.4% of the BTEX mass determined for the calibrated model. This suggests that the results in the calibrated model contain considerable uncertainty, caused in term by uncertainty in the hydraulic conductivity field.

The relationships among BTEX, electron acceptors and reduced products, follow some general trends. More BTEX mass in the aquifer results in either a large depletion

of DO and NO_3^- mass or large depletion of DO and Fe^{2+}. A plume with low BTEX mass corresponds to a smaller depletion of DO and Fe^{2+} compared to the calibrated model. The shape of the BTEX plume is mainly controlled by longitudinal elongation. A more elongated plume tends to have a narrower transverse width, leading to a "channelization" of the plume. An elongated, or channelized, plume helps BTEX travel farther longitudinally, but it is not favorable for transverse spreading, thus leading to lower BTEX mass in the aquifer. On the other hand, plumes with larger BTEX mass are generally related to those skewed to the upper (southeastern) side of the flow field. This is resulted from a generally lower hydraulic gradient near the lower side of the flow field, caused by a relatively higher elevation near borehole CPT 33 (Figure 1).

The variance and correlation length of the random hydraulic conductivity field is varied to investigate their effect on the fate and transport of BTEX and other species. An increase in variance results in a higher average BTEX mass in the aquifer, whereas an increase in correlation length results in a lower average BTEX mass in the aquifer. The results of multispecies reactive transport modeling are clearly affected by the varying degrees of heterogeneity and uncertainty in the aquifer's physical properties. These observations may have been contributed by the BTEX source from LNAPL, from which the BTEX mass partitioning is more realistically modeled by constant-concentration cells.

This study has examined the impact of spatial K variability and associated uncertainty on the fate and transport of BTEX compounds reacting with multiple electron acceptors. This study represents a well-controlled numerical experiment to quantify the complete sequence of BTEX natural attenuation processes at a field site in

the presence of uncertain hydraulic conductivity. Although the findings from this study may be applicable only to the field conditions considered in this study, the methodology used and insights gained are of general interest and relevance to other fuel-hydrocarbon natural attenuation sites.

Acknowledgments

The authors thank T. P. Clement (University of Western Australia) for his comments, E. A. Sudicky (University of Waterloo), P. Wang (Dept. of Mathematics, University of Alabama), H. C. Chen (Dept. of Computer Science, University of Alabama), and D. Zhang (Los Alamos National Laboratory) for their suggestions on this research project, and Dan Hawkes for his editorial improvement of the manuscript.

References

Bekins, B.A., Rittmann, B.E., MacDonald, J.A., 2001. Natural attenuation strategy for groundwater cleanup focuses on demonstrating cause and effect, *Eos, Transactions, Am. Geophys. Uni.* 82(5), 53-58.

Borden, R.C., Daniel, R.A., LeBrun IV, L.E., Davis, C.W., 1997. Intrinsic biodegradation of MTBE and BTEX in a gasoline-contaminated aquifer. *Water Resour. Res.* 33 (5), 1105-1115.

Brauner, J.S., Widdowson, M.A., 2001. Numerical simulation of a natural attenuation experiment with a petroleum hydrocarbon NAPL source. *Ground Water* 39 (6), 939-952.

Clement, T.P., 1998. A modular computer model for simulating reactive multi-species transport in three-dimensional ground water systems. Pacific Northwest National Laboratory, PNNL-SA-11720. Richland, Washington: PNNL.

Essaid, H.I., Bekins, B.A., Godsy, E.M., Warren, E., Baedecker, M.J., Cozzarelli, I.M., 1995. Simulation of aerobic and anaerobic biodegradation processes at a crude oil spill site. *Water Resour. Res.* 31 (12), 3309-3327.

James A.L., Oldenburg, C.M., 1997. Linear and Monte Carlo uncertainty analysis for subsurface contaminant transport simulation. *Water Resour. Res.* 33 (11), 2495-2508.

Lu, G., Clement, T.P., Zheng, C., Wiedemeier, T.H., 1999. Natural attenuation of BTEX compounds: Model development and field scale-application. *Ground Water* 37 (5), 707-717.

McDonald, M.G., Harbaugh, A.W., 1988. A Modular Three-Dimensional Finite Difference Groundwater Flow Model. U.S. Geological Survey Techniques of Water Resources Investigations, Book 6, 586 pp.

MacQuarrie, K.T.B., Sudicky, E.A., 1990. Simulation of biodegradable organic contaminants in groundwater 2. Plume behavior in uniform and random flow fields. *Water Resour. Res.* 26 (2), 223-239.

National Research Council (NRC), 2000. Natural Attenuation for Groundwater Remediation, National Academy Press, Washington, DC., 292 p.

Patrick, G. C., 1986. A natural gradient tracer experiment of dissolved benzene, toluene and xylenes in a shallow sand aquifer. M.S. thesis, University of Waterloo, Waterloo, Ont., Canada.

Schumm, S.A., 1956. Evolution of drainage systems and slopes in badlands at Perth Amboy, New Jersey. *Geol. Soc. Amer. Bull.* 67, 597-646.

U.S. EPA, 1997. Use of monitored natural attenuation at superfund RCRA, and underground storage tank sites. Directive no. 9200.4-17, OSWER report.

Widdowson, M.A., Molz, F.J., Benefield, L.D., 1987. Development and application of a model for simulating microbial growth dynamics coupled to nutrient and oxygen transport in porous media, paper presented at the NWWA Conference on Solving Ground Water Problems With Models, Natl. Water Well Assoc., Denver, Colo.

Wiedemeier, T., Wilson, J.T., Kampbell, D.H., Miller, R.N., Hansen, J.E., 1995. Technical protocol for implementing intrinsic remediation with long-term monitoring for natural attenuation of fuel contamination dissolved in groundwater (Volume II). Air Force Center for Environmental Excellence Technology Transfer Division, Brooks AFB, San Antonio, Texas.

Zadeh, L.A, 1968. Probability measures of fuzzy events. Journal of mathematical analysis and applications 23, 421-427.

Zheng, C., 1990. MT3D: A modular three dimensional transport model for simulation of advection, dispersion and chemical reactions of contaminants in groundwater systems. Report to the U.S. Environmental Protection Agency, Ada, OK, 170pp.

Zimmerman, D.A., Wilson, J.L., 1990. Description of and user's manual for TUBA: A computer code for generating two-dimensional random fields via the turning bands method, Scientific & Engineering Analysis Software and Engineering Consulting, Albuquerque, New Mexico, 116pp.

Table 1. Hydraulic conductivity values from slug tests (modified from Wiedemeier et al., 1995).

Well	Test	Hydraulic Conductivity (m/day)	
		K	lnK
EPA-82-A	Rising head #1	0.31	-1.16
	Rising head #2	0.13	-2.04
	Rising head #3	0.16	-1.86
EPA-82-E	Rising head #1	14.43	2.67
EPA-82-E	Rising head #2	15.98	2.77
EPA-82-F	Rising head #1	3.57	1.28
EPA-82-F	Rising head #2	2.83	1.04
EPA-82-H	Rising head #1	6.53	1.88
EPA-82-H	Rising head #2	7.19	1.97
EPA-82-I	Rising head #1	4.13	1.42
EPA-82-I	Rising head #2	0.943	-0.06
Mean		7.02	0.96
Variance		25.46	2.73

Table 2. Statistical parameters of the random hydraulic conductivity field used in the first analysis (Base Case).

Parameters	Value (lognormal field)
Mean	0.96 m/day
Nugget	0.0 m/day
Sill	2.73 m/day
Variance[a]	2.73 m/day
Correlation length	
x-direction	134.1 m (440 ft)
y-direction	103.6 m (340 ft)

[a] variance = sill + nugget

Table 3. Statistics of calculated masses for the Monte Carlo simulation expressed in terms of the percentage of mass difference from the calibrated model)[a]

	BTEX	DO	nitrate	Ferric iron	sulfate	methane
Range	-12.0~60.4	-67.9~88.0	-72.9~18.3	-73.7~71.8	-45.5~88.9	-31.7~22.0
Mean	9.8	-15.2	-16.5	14.1	-5.4	0.9
Standard Deviation	13.9	19.3	13.7	21.5	15.2	8.5

[a]count = 120

Figure Captions

Figure 1. Plan view of POL Site on Hill Air Force Base (AFB), Utah with the positions of observation wells (modified from Lu et al., 1999).

Figure 2. Hydrologic section A-A' for the Hill AFB site with datum at 4000 ft mean sea level (msl) (modified from Lu et al., 1999).

Figure 3. Histogram of calculated total BTEX masses dissolved and remaining in the aquifer at the end of one-year simulation period for the base case (120 realizations).

Figure 4. Histogram of calculated BTEX plume areas (120 realizations) (plume outer limit set to 0.05 mg/L contour line).

Figure 5. Histogram of BTEX plume longitudinal elongation ratios (R_{el}) (120 realizations).

Figure 6. Histogram of BTEX plume transverse elongation ratios (Ret) (120 realizations)

Figure 7. Histogram of BTEX plume shape ratios (120 realizations)

Figure 8. Diagram of BTEX plume area vs. coefficient of skewness (relative to the central axis, along flow direction, of the calibrated BTEX plume).

Figure 9. A decision tree for the relationship assessment of total BTEX mass with DO, NO_3^-, and Fe^{2+} in the aquifer. DO, NO_3^-, and Fe^{2+} are grouped according to their mass differences with respect to their corresponding calibrated masses. Total BTEX mass is grouped into three categories: high (total BTEX mass ≥37 kg), low(<34 kg), medium (≥ 34 and <37 kg). The first feature used for classification of BTEX is "DO difference", divided into three categories: large (difference ≥ 100 kg), small (<30 kg), medium (≥ 30 and <100 kg). The classification with "NO_3^- difference" also employs three categories: large (difference ≥ 90 kg), small (<30 kg), medium (≥ 30 and < 90 kg). The grouping by "Fe^{2+} difference" is based on two categories: large (difference ≥ 100 kg), small (<100 kg).

Figure 10. Calculated means and variances of the BTEX mass remaining in the aquifer at the end of the one-year simulation period, as a function of the variance and correlation length of the random hydraulic conductivity field for 2400 realizations (Extended Case).

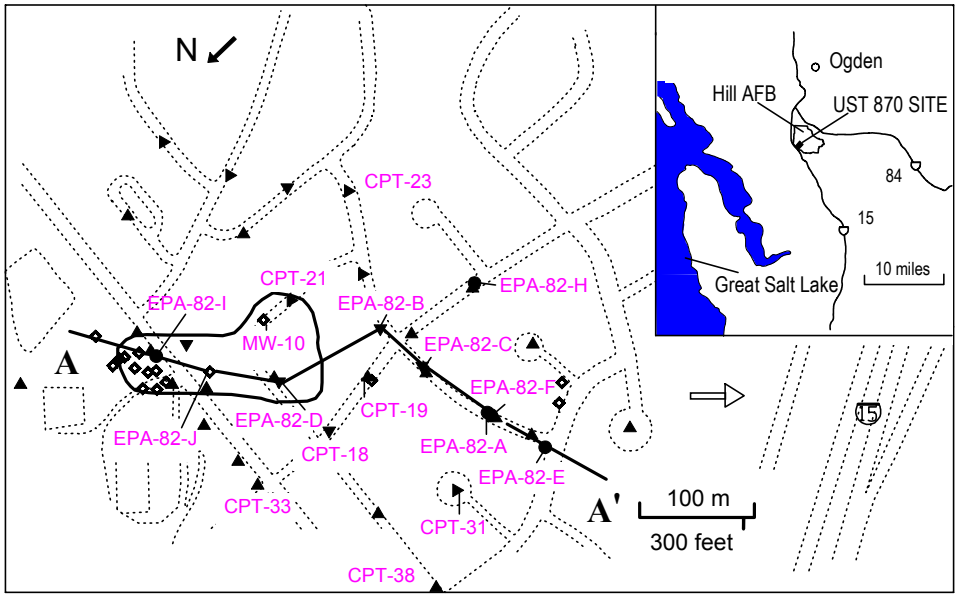
N
CPT-23
CPT-21
EPA-82-I
EPA-82-B
EPA-82-H
MW-10
EPA-82-C
A
EPA-82-F
CPT-19
EPA-82-D
EPA-82-J
CPT-18
EPA-82-A
EPA-82-E
CPT-33
CPT-31
A'
CPT-38
100 m
300 feet
Ogden
Hill AFB
UST 870 SITE
84
15
Great Salt Lake
10 miles
15
slug test well location
flow calibratrion well location
monitoring well location
monitoring flow calibration well location
piezometer
LNAPL plume (July/August 1993)
regional flow direction

Figure 1

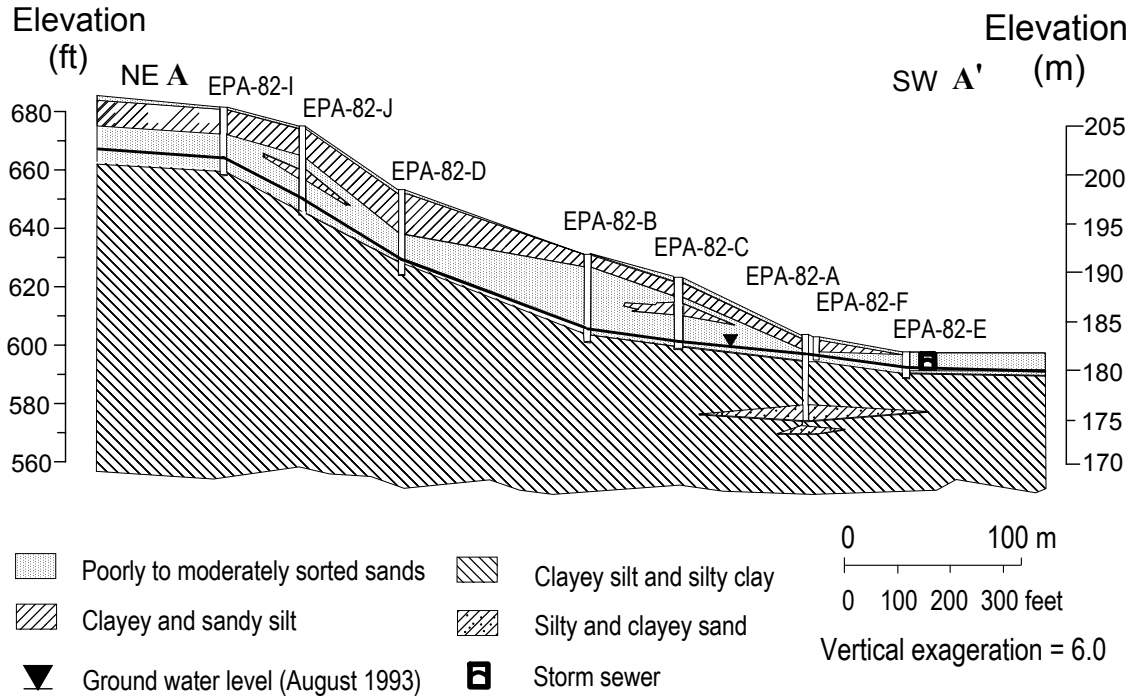
Elevation
(ft)
NE A
A'
SW
Elevation
(m)
EPA-82-I
EPA-82-J
EPA-82-D
EPA-82-B
EPA-82-C
EPA-82-A
EPA-82-F
EPA-82-E
680
660
640
620
600
580
560
205
200
195
190
185
180
175
170
0
100 m
0 100 200 300 feet
Vertical exageration = 6.0
Poorly to moderately sorted sands
Clayey and sandy silt
Ground water level (August 1993)
Clayey silt and silty clay
Silty and clayey sand
Storm sewer

Figure 2

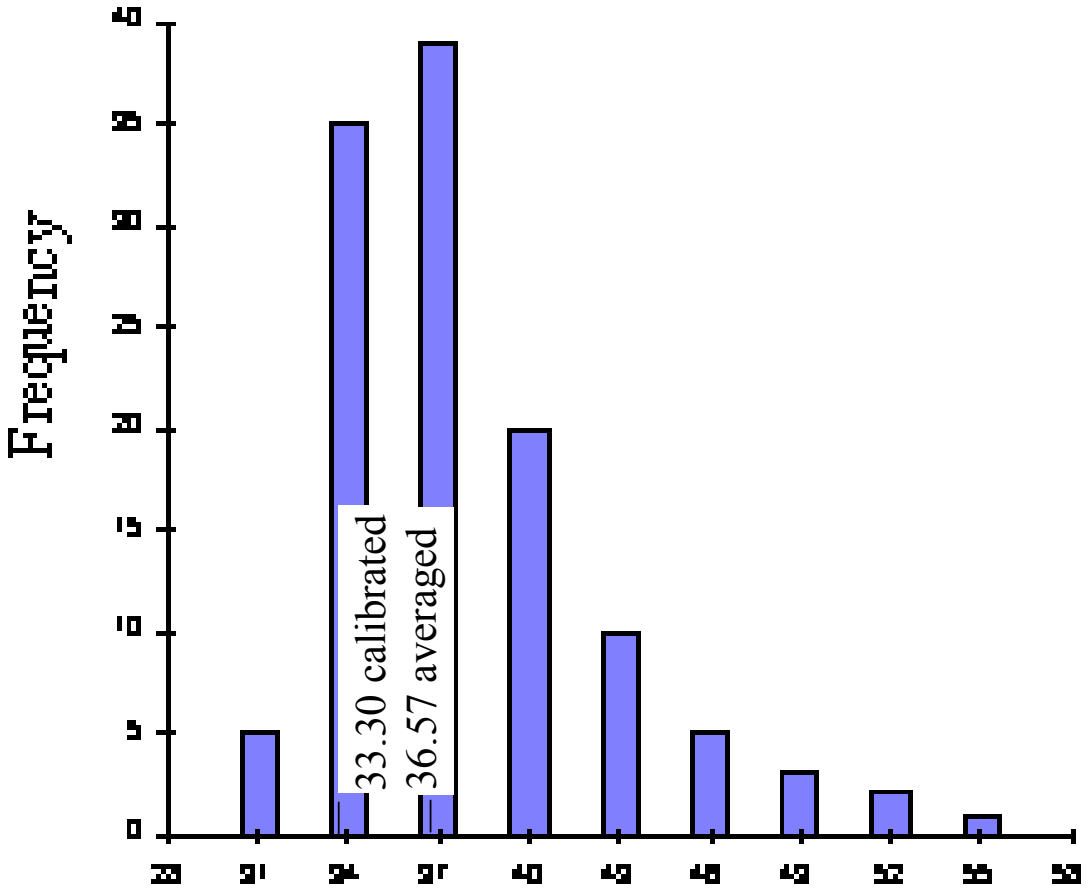
Frequency
33.30 calibrated
36.57 averaged
Total mass of BTEX dissolved in the aquifer (kg)

Figure 3

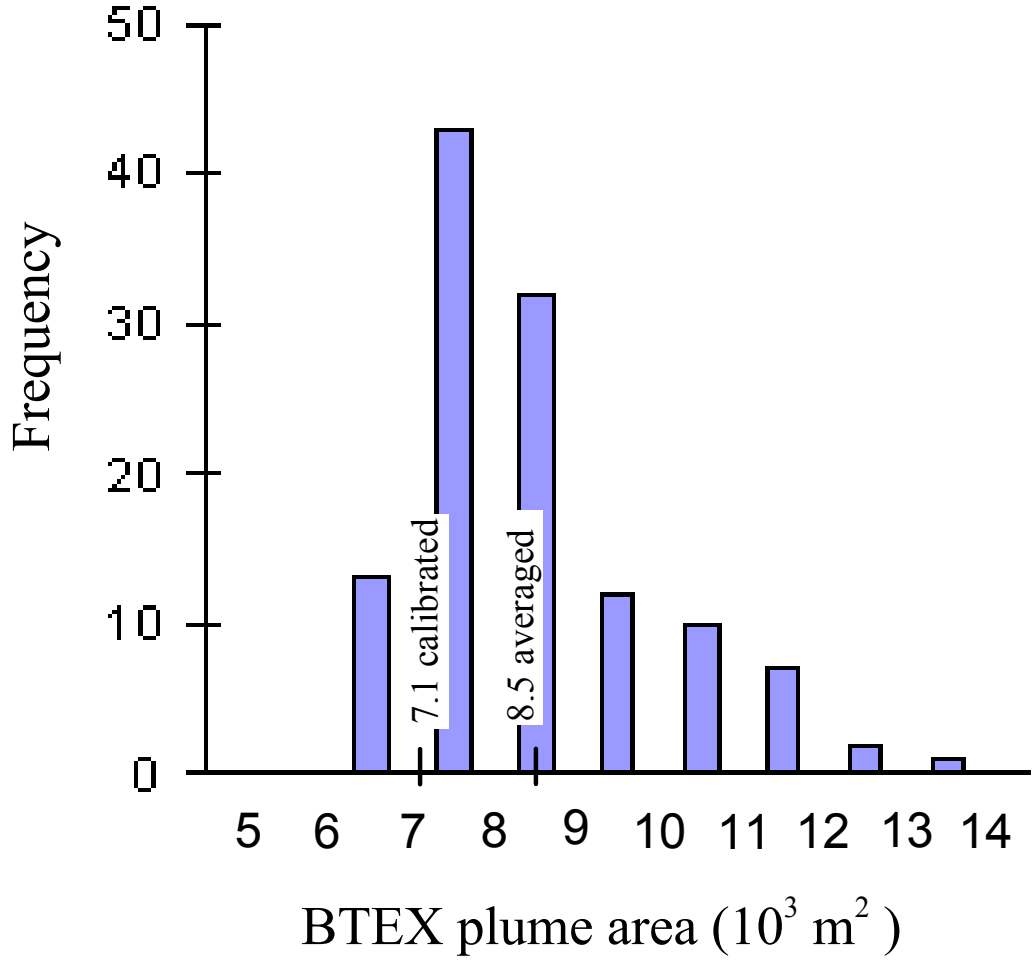
Frequency
50
40
30
20
10
0
7.1 calibrated
8.5 averaged
5
6
7
8
9
10
11
12
13
14
BTEX plume area (10^3 m^2)

Figure 4

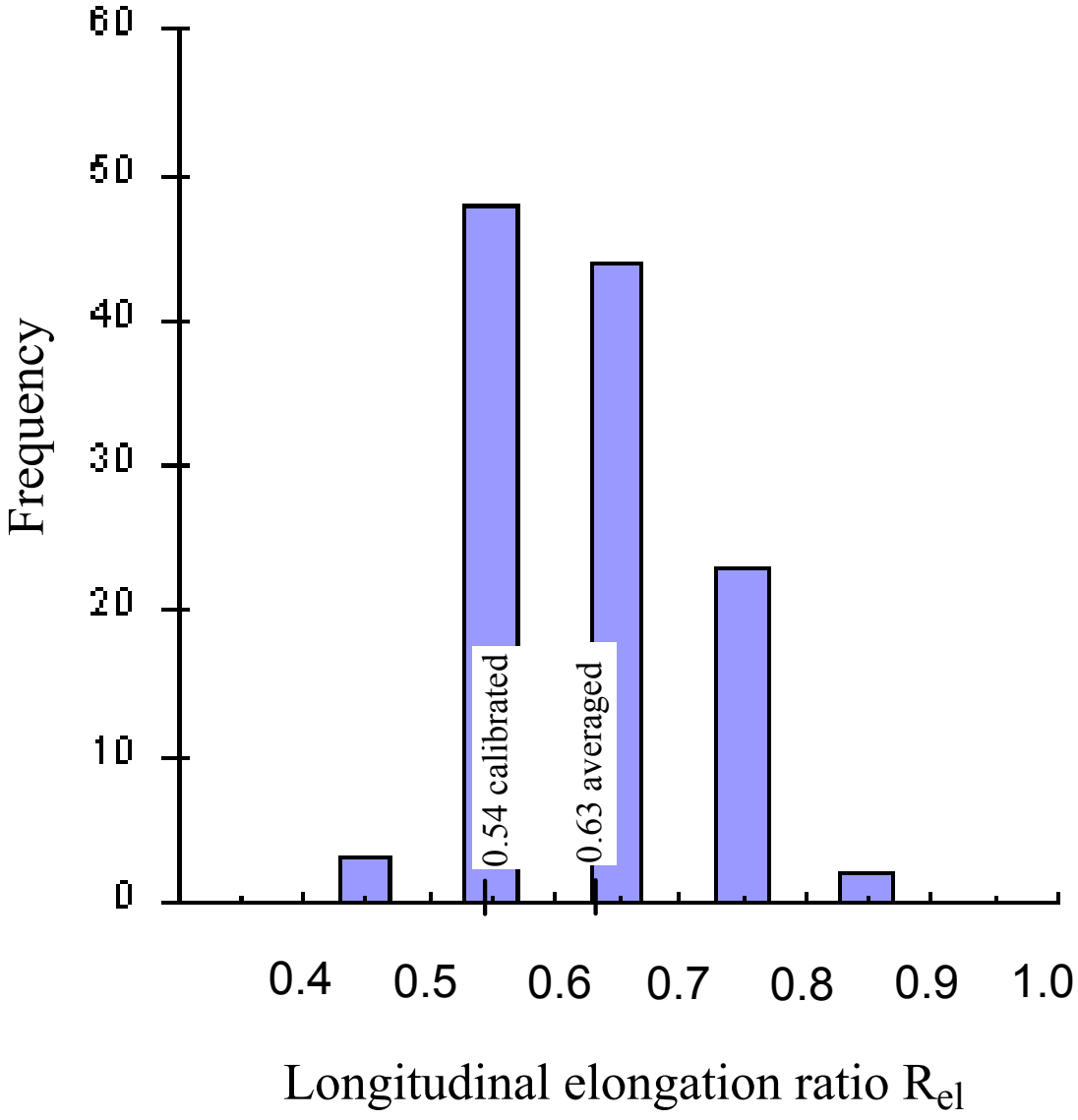
60
50
40
30
20
10
0
Frequency
0.54 calibrated
0.63 averaged
0.4
0.5
0.6
0.7
0.8
0.9
1.0
Longitudinal elongation ratio R_{el}

Figure 5

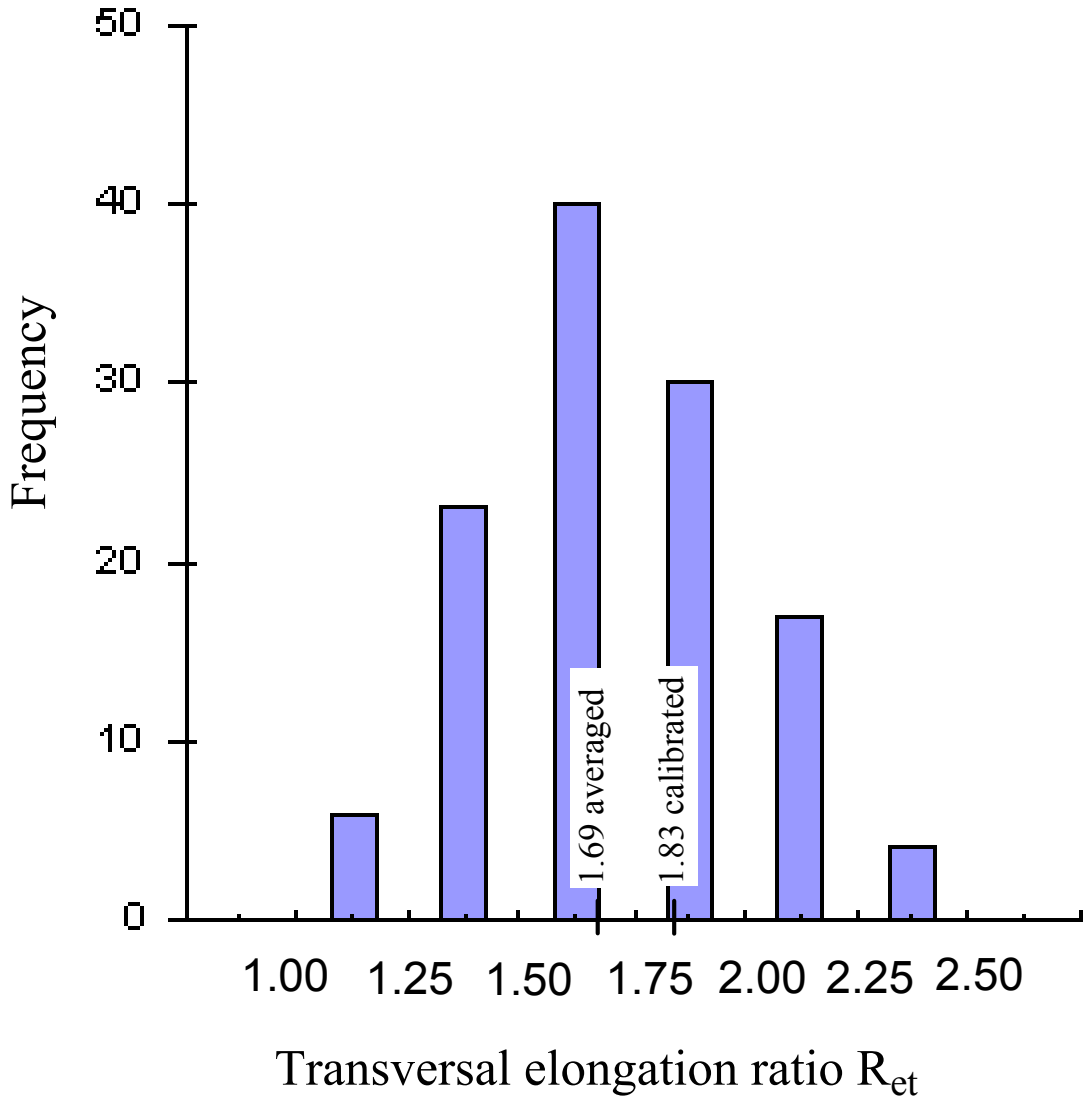
50
40
30
20
10
0
Frequency
1.69 averaged
1.83 calibrated
1.00
1.25
1.50
1.75
2.00
2.25
2.50
Transversal elongation ratio R_{et}

Figure 6

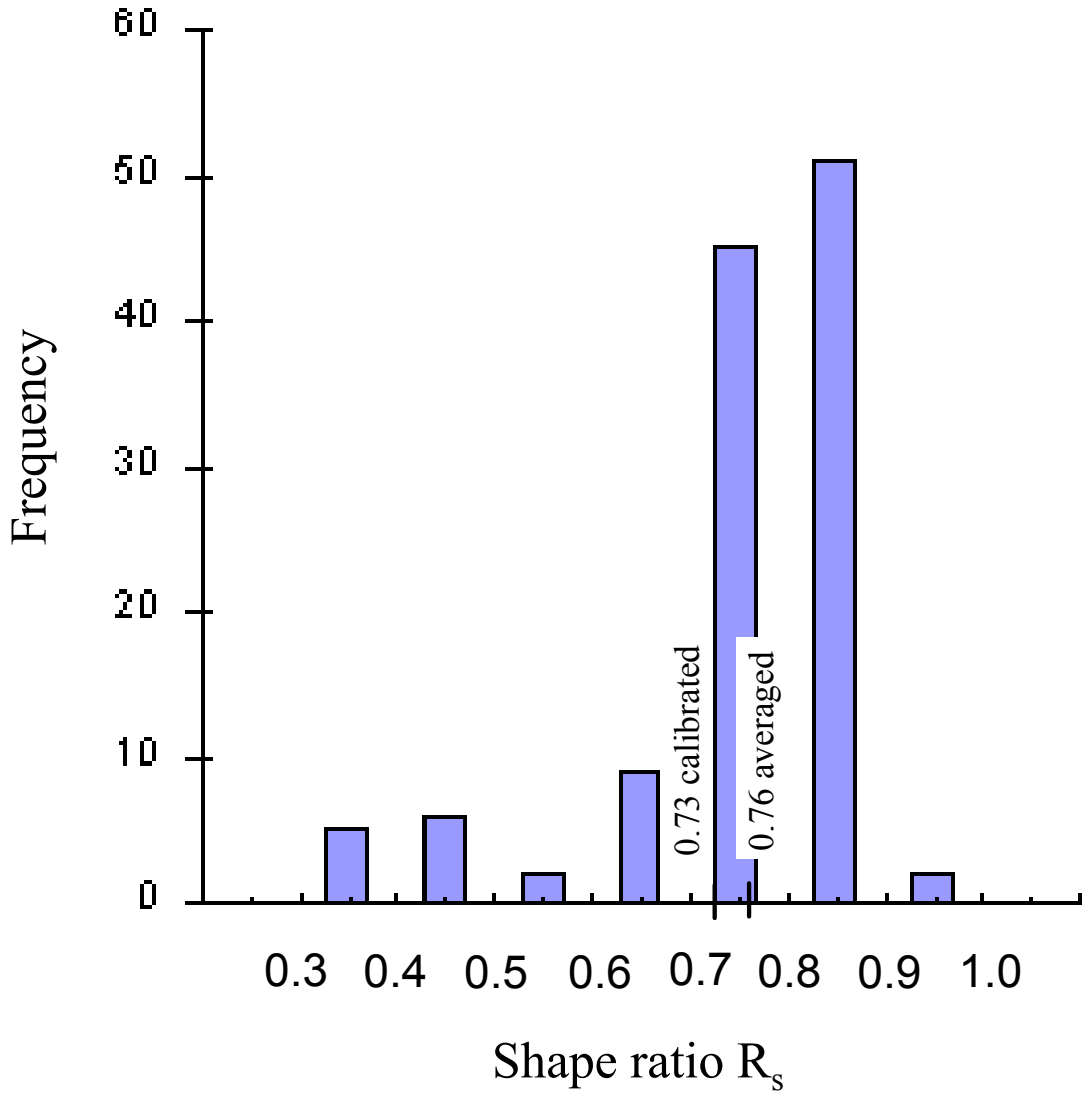
60
50
40
30
20
10
0
Frequency
0.73 calibrated
0.76 averaged
0.3
0.4
0.5
0.6
0.7
0.8
0.9
1.0
Shape ratio R_s

Figure 7

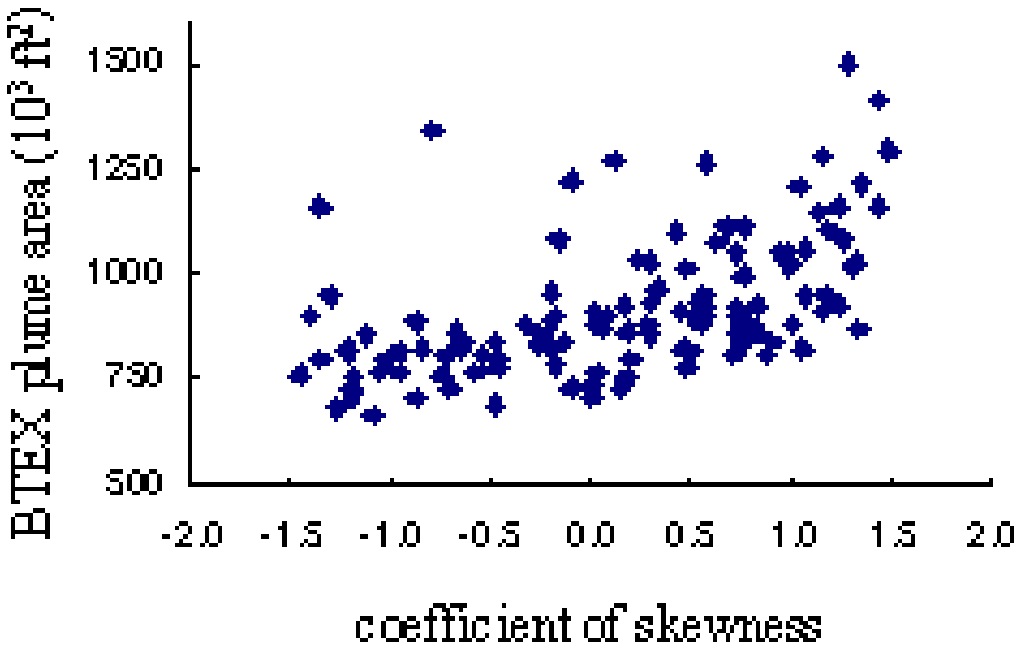
BTEX plume area (10³ ft²)
1500
1250
1000
750
500
-2.0
-1.5
-1.0
-0.5
0.0
0.5
1.0
1.5
2.0
coefficient of skewness

Figure 8

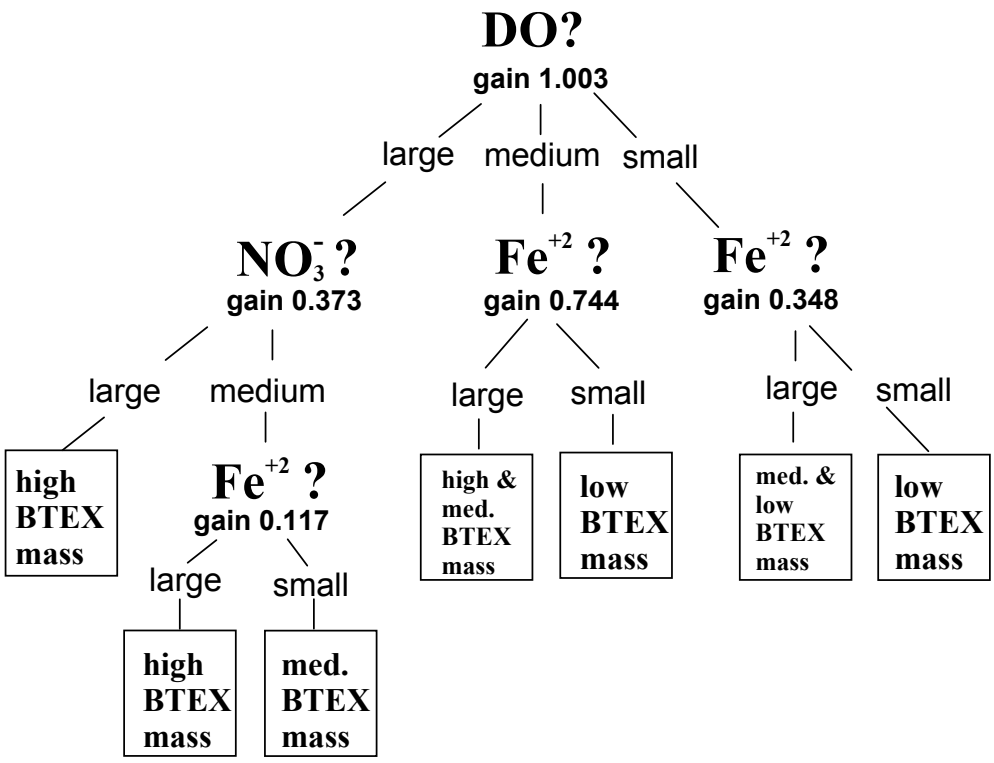
DO?
gain 1.003
large
medium
small
NO3- ?
gain 0.373
Fe+2 ?
gain 0.744
Fe+2 ?
gain 0.348
large
medium
large
small
large
small
high BTEX mass
Fe+2 ?
gain 0.117
high & med. BTEX mass
low BTEX mass
med. & low BTEX mass
low BTEX mass
large
small
high BTEX mass
med. BTEX mass

Figure 9

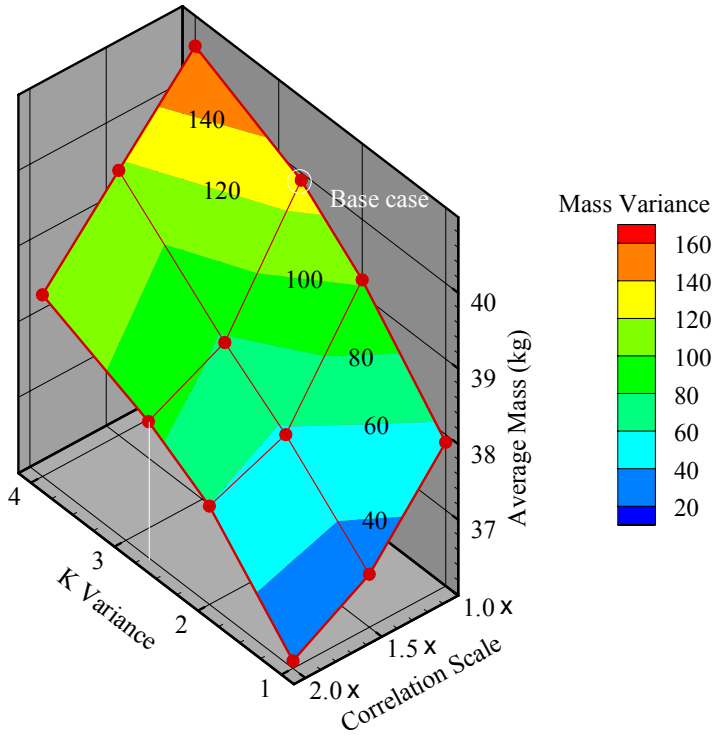
140
120
100
80
60
40
Base case
40
39
38
37
Average Mass (kg)
4
3
2
1
K Variance
1.0 x
1.5 x
2.0 x
Correlation Scale
Mass Variance
160
140
120
100
80
60
40
20

Fig. 10